

Trends in Precipitable Water and Relative Humidity in China: 1979–2005

BAOGUO XIE, QINGHONG ZHANG, AND YUE YING

Department of Atmospheric and Oceanic Science, School of Physics, Peking University, Beijing, China

(Manuscript received 7 December 2009, in final form 8 April 2011)

ABSTRACT

Annual and seasonal trends of precipitable water (PW) and relative humidity (RH) at 850, 700, and 500 hPa are studied using the data from 106 radiosonde stations over China during the period 1979–2005. Analysis shows evidence of an increase in PW associated with the slight warming observed in the lower to mid-troposphere over China. The northern part of China shows a significant upward trend of PW in summer, and drying of the atmosphere in winter is found in most regions over China. Annual and seasonal trends in RH at the 850-, 700-, and 500-hPa levels show no significant trends in most regions in China except for Xinjiang, which shows an upward trend, and central China, where there was a downward trend in RH at 500 hPa. It is found that changes in PW are coincident with the warming of the surface and the lower to midtroposphere. The RH in the lower to midtroposphere in most regions over China has remained steady during the most recent 30 years, as might be expected given the increasing of PW and the warming above the surface. The long-term trend of precipitation over China may be linked to the trends of PW and RH at the lower level and midlevel.

1. Introduction

Water vapor plays an important role in large-scale atmospheric circulation as well as in global water and energy cycles. In the lower troposphere, water vapor acts as the main resource for precipitation in all weather systems, providing latent heating in the process (Trenberth and Stepaniak 2003a,b). Trenberth (1999) indicated that, for extratropical cyclones, on average about 70% of the precipitation comes from moisture that was already in the atmosphere at the time that the storms formed. With climatic warming, the amount of moisture in the atmosphere is expected to increase much faster than the total precipitation amount. The latter is dominated by the surface heat budget through evaporation in the areas where water availability is not limiting. Atmospheric moisture is expected to rise with temperature (Trenberth et al. 2003). Therefore, water vapor, especially precipitable water (PW), is very important for understanding global and regional climatic changes. The Intergovernmental Panel on Climate Change report from 2007 presents the general research about the trends of global and regional

water vapor, which implies that global warming increases saturation vapor pressure and hence enables the increase of moisture in the atmosphere.

Water vapor is also the most important greenhouse gas in the atmosphere, accounting for about 60% of the natural greenhouse effect for clear skies (Kiehl and Trenberth 1997). It provides the largest positive feedback in numerical model projections of climatic change (Held and Soden 2000).

Relative humidity (RH), according to its definition, is an indication of the amount of water vapor that is present relative to that which the air can “hold” at a given temperature (the saturation vapor pressure). Changes in RH in lower levels of atmosphere are very critical, since low-level RH is closely related to the hydrological processes (precipitation, condensation, and evaporation) and the surface energy exchanges. The variations in RH (relative measure of moisture amount) after the 1980s and in PW (absolute measure of moisture amount) are both essential for understanding the changes in atmospheric water content and precipitation involved with current climatic changes and for reducing uncertainties for estimating future climatic changes.

Worldwide research efforts have together noted the increase of atmospheric water vapor both at the surface (Elliott 1995; Dai 2006; Willett et al. 2008; Robinson 2000; Philipona and Dürr 2004; Philipona et al. 2005;

Corresponding author address: Dr. Qinghong Zhang, Dept. of Atmospheric and Oceanic Sciences, School of Physics, Peking University, Beijing 100871, China.
E-mail: qzhang@pku.edu.cn

Wang and Gaffen 2001) and aloft (Trenberth et al. 2005; McCarthy et al. 2009). Radiosonde observations showed an increasing trend in surface–500-hPa water vapor in the Western Hemisphere north of the equator from 1973 to 1993 (Ross and Elliott 1996) and further for the whole Northern Hemisphere from 1973 to 2006 (Durre et al. 2009). Dai (2006) found that trends in specific humidity with 60°S–75°N ship and buoy data of 1976–2005 were consistent with surface temperature data. Evidence from Special Sensor Microwave Imager (SSM/I) global ocean data suggests that recent trends in PW are generally positive, with an average of $0.40 \pm 0.09 \text{ mm (10 yr)}^{-1}$ for 1988–2003 (Trenberth et al. 2005). Using the analysis data from the Met Office Hadley Centre and Climatic Research Unit Global Surface Humidity dataset (HadCRUH), an increasing trend in the specific humidity at the surface and aloft was found over the globe, tropics, and Northern Hemisphere after the 1970s (Willett et al. 2008; McCarthy et al. 2009).

Regional data from North America (Robinson 2000; Wang et al. 2008), Europe (Philipona and Dürr 2004; Philipona et al. 2005), the North Atlantic Ocean (Trenberth et al. 2005), and eastern Asia (Zhai and Eskridge 1997; Wang and Gaffen 2001) have consistently documented the increase of atmospheric water vapor. Most studies have confirmed that such an increase was strongly coupled to the surface temperature, with regions of warming (cooling) observing increasing (decreasing) moisture. Former studies in eastern Asia focused on the period of 1970–90. The variability and trends of PW in China after the 1990s have not yet been examined, however.

The global trends of near-surface RH are very small, and nighttime RH is greater than daytime RH by 2%–15% over most continental areas (Dai 2006). This result is similar to the recent finding that lower-tropospheric temperature has increased with RH holding steady in the United States (Wang et al. 2008). Nevertheless, western China, as well as the United States and India, showed a significant positive trend in surface RH (Dai 2006). Willett et al. (2008) also reported that changes in RH were not significant except for some seasonal changes over the globe, tropics, and Northern Hemisphere from 1973 to 2003. Another study documented a reduction in RH at the surface over lower to mid-latitudes in continental areas over a 10-yr period up to 2008 (Simmons et al. 2010). They concluded that the limited moisture supplied by oceans is responsible for such a reduction. The behavior of RH in the lower to midtroposphere over China during recent climatic change is a remaining question.

This article further studied the distribution, annual and seasonal variability, and trends of PW in the lower troposphere to midtroposphere over China during

1979–2005 and attempted to understand the variations in corresponding RH values. The data analysis and method are presented in section 2. Climatological means of PW and RH are described in section 3, and the long-term annual and seasonal variations and trends of PW and RH in different regions are presented in section 4, which is followed by a discussion in section 5. A summary is given in section 6.

2. Data and method

The detection of changes in water vapor as a feedback of temperatures is not easy to perform because of inaccuracy in measurements and difficulty in data collection. Elliott (1995) emphasized that the radiosonde observations provided the longest record but with many uncertainties and much bias. McCarthy et al. (2008, 2009) proposed a new method in processing radiosonde data that could produce results that are similar to those of subjective analysis. The uncertainties and bias are significantly reduced within the concern of linear trends using such method. The Climate Change Science Program and the Subcommittee on Global Change Research have developed the Synthesis and Assessment Product, which also aimed to eliminate the discrepancies between the surface observations and atmospheric data on global-average warming (Karl et al. 2006). Above all, radiosonde observations are the most reliable datasets available for long-term analysis of changes in atmospheric water vapor.

The data used in this study are obtained from a real-time data feed using the Global Telecommunications System (GTS) under the World Meteorological Organization. It is open source with free access and covers a 27-yr period (1979–2005) with 120 stations' radiosonde observations. Soundings profiles moved from GTS always have inevitable errors, and a quality-control (QC) process is necessary. The QC method contains three steps. First, we discard obvious gross errors from the data. Values of PW of less than 100 kg m^{-2} and temperatures and dewpoint temperature within $\pm 100^\circ\text{C}$ are considered to be valid and are passed on to the next step. Second, the annual and monthly mean values for each station are calculated based on outputs from the first step. Statistics are performed on PW, temperature, and dewpoint temperature values, and expectations μ and standard deviations σ are computed with the daily means. The datasets are then filtered using a criterion that each variable be within a $\mu \pm 5\sigma$ range. Note that the systematic and instrumental errors are not under consideration in the QC process.

The semifinal datasets are further tested for inhomogeneity in the following procedure: 1) Data from

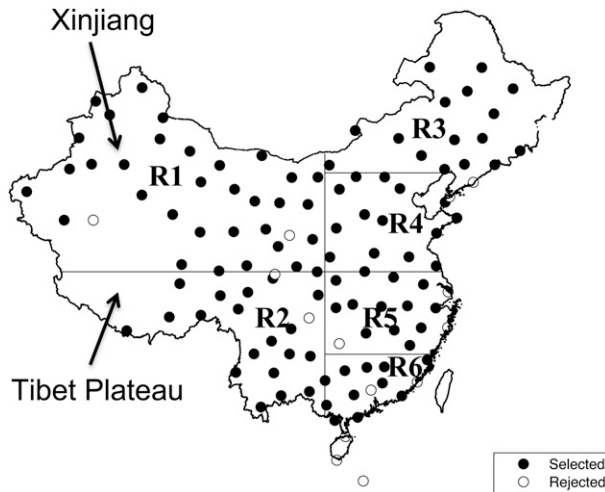


FIG. 1. The definition of six regions and stations selected (filled circles) and rejected (open circles) for this study. The six regions are R1: northwestern China; R2: southwestern China; R3: northeastern China; R4: northern China; R5: central China; R6: southern China.

stations with obvious inhomogeneity are excluded. 2) Data from relocated stations are excluded. 3) Data from stations without complete twice-daily observations at 0000 and 1200 UTC are excluded. 4) To ensure the reliability of the analysis result, at least 15 observations are used to calculate the mean monthly values, although Gaffen et al. (1991) and Zhai and Eskridge (1997) obtained mean monthly value by using only three observations for a month. A month with observations on fewer than 15 days is defined as an invalid month. In addition, only a year that has at least eight valid months is qualified to be used to derive the annual and seasonal mean values. 5) Data from stations without a consistent time series of 1979–2005 annual mean observations are excluded. The inhomogeneity test showed that there are no severe inconsistencies in our datasets from 1979 to 2005. The major cause of inhomogeneities is the relocation of some stations. Therefore, the datasets are good enough for our analysis. These test results are consistent with reliability tests done by Zhai and Eskridge (1997). After the QC and inhomogeneity-test procedures, 106 out of 120 stations are selected for our study (Fig. 1), but, because of the high elevation of some stations in the Tibet area, the total numbers of stations used in PW and RH analysis have a slight difference.

The PW, geopotential height, temperature, and dewpoint temperature are extracted from the dataset directly. In this paper, PW is calculated from integration of water vapor mass through all levels of the sounding. Temperature, dewpoint temperature, and the corresponding pressure values are used to calculate RH on each level.

Because Zhai and Eskridge (1997) have pointed out that humidity is not recorded when temperature is below -60° or pressure is less than 10 hPa, only RH at 850, 700, and 500 hPa are computed. Such a selection of levels still captures the characteristics of atmospheric water content, considering the fact that water vapor is concentrated in the lower troposphere to midtroposphere (Elliott 1995). To measure the changes in free-atmosphere temperature (FAT), the thickness between the 850- and 500-hPa surfaces is calculated from the geopotential height values, instead of calculating the mean atmosphere temperature:

$$\Delta H \equiv H_{500} - H_{850} = -\frac{R_d}{g_0} \int_{850}^{500} T d \ln p. \quad (1)$$

In Eq. (1), R_d is the universal gas constant, g_0 is gravity acceleration, T is air temperature at pressure levels, and p is pressure. Therefore, thickness ΔH is a good measurement of mean FAT. Surface temperature (SFT) is also included in the analysis.

The dataset contains twice-daily radiosonde observations at 0000 and 1200 UTC. Ross and Elliott (1996) showed that there was no substantial difference in trend between 0000 and 1200 UTC at the pressure levels presented. On the basis of this consideration, the two observations each day are averaged to derive daily mean values.

Annual and seasonal variations and trends of analysis fields are calculated on the basis of the monthly and annual mean. Trends of PW and RH in winter and summer are shown to illustrate the seasonal variation; results of spring and autumn are not shown because of their respective similarity to those of winter and summer. The magnitude of trends is calculated for the entire 1979–2005 period. To evaluate the variability and trends of PW and RH in different regions, we divide China into eastern and western regions with a boundary along 107.5°N . We further divide western China into two regions (along 30°N , also known as the Yangtse–Qinling–Huai geographic line) and eastern China into four regions (northeastern, northern, central, and southeastern China). The six regions are shown in Fig. 1. In the following text, the northern part of China refers to the northwestern, northeast, and northern China regions and the southern part of China refers to the southwestern, central, and southern China regions.

The least squares linear regression method was employed to estimate trends in this study. The parametric method is based on finding the equation of best fit to time series data (annual or seasonal mean values) by minimizing the sum of the squares of the errors in the residuals. For each trend estimation, the 95% confidence interval of the trend as a function of the trend estimate is calculated. The significance of each trend fit is also calculated to judge

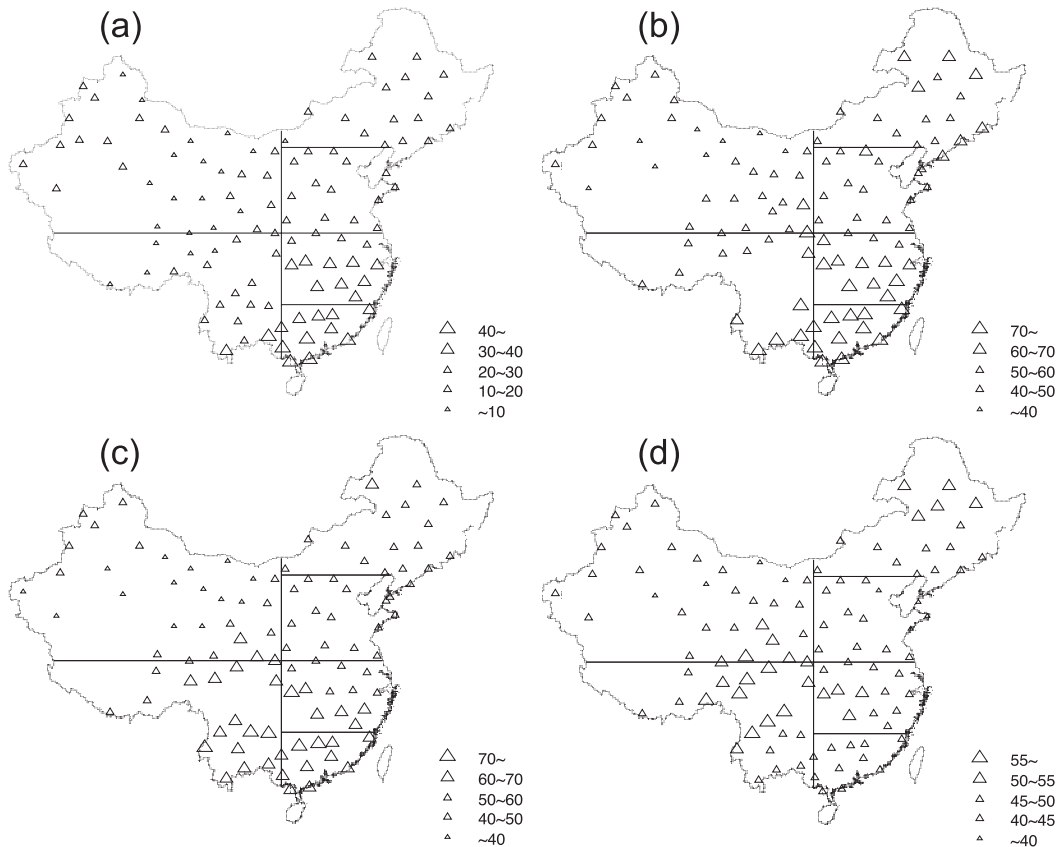


FIG. 2. Spatial distribution of (a) PW (kg m^{-2}) and RH (%) at (b) 850, (c) 700, and (d) 500 hPa averaged over the period of 1979–2005.

the regression effect on the basis of the 95% confidence level. Representativeness issues of each station are not considered in the calculation of regional means, since the distribution of stations in China is spatially homogeneous enough except for only a few stations on the Tibetan Plateau (Fig. 1).

3. Climatological means

Spatial distributions of PW and RH are essential to understanding their temporal variations. On the basis of the 27-yr data from 1979 to 2005, the mean fields of PW and RH are presented to offer a context for the trend analysis that follows.

a. PW

Figure 2a shows the spatial variations of PW averaged over the 1979–2005 period. It is clear that the PW-decreasing distribution pattern orients generally from southeast to northwest over China. The mean PW over China is 19.50 kg m^{-2} , and southern China has six stations with PW greater than 40 kg m^{-2} . Central China, which is the second wettest region in China, has PW of

$30\text{--}40 \text{ kg m}^{-2}$. The PW in northern China and north-eastern China are similar to each other, with values lying between 10 and 20 kg m^{-2} .

b. RH

The climatological mean distributions of RH at the 850-, 700-, and 500-hPa levels are given in Figs. 2b–d, respectively. Like PW, the distribution of RH is mainly affected by elevation and geographic location (Zhai and Eskridge 1997). There is an overall decrease of RH with respect to height. The RH at the three levels all roughly increases from north to south over China, with the highest RH values lying along the coast. It is clear that the RH pattern at 850 hPa is similar to that at 700 hPa. Meanwhile, there is smaller variability in RH at the midtropospheric level than that at lower levels with respect to geographic location.

4. Trends and variations

To find out the trends of PW and RH during 1979–2005, annual and seasonal mean PW and RH are calculated for each station.

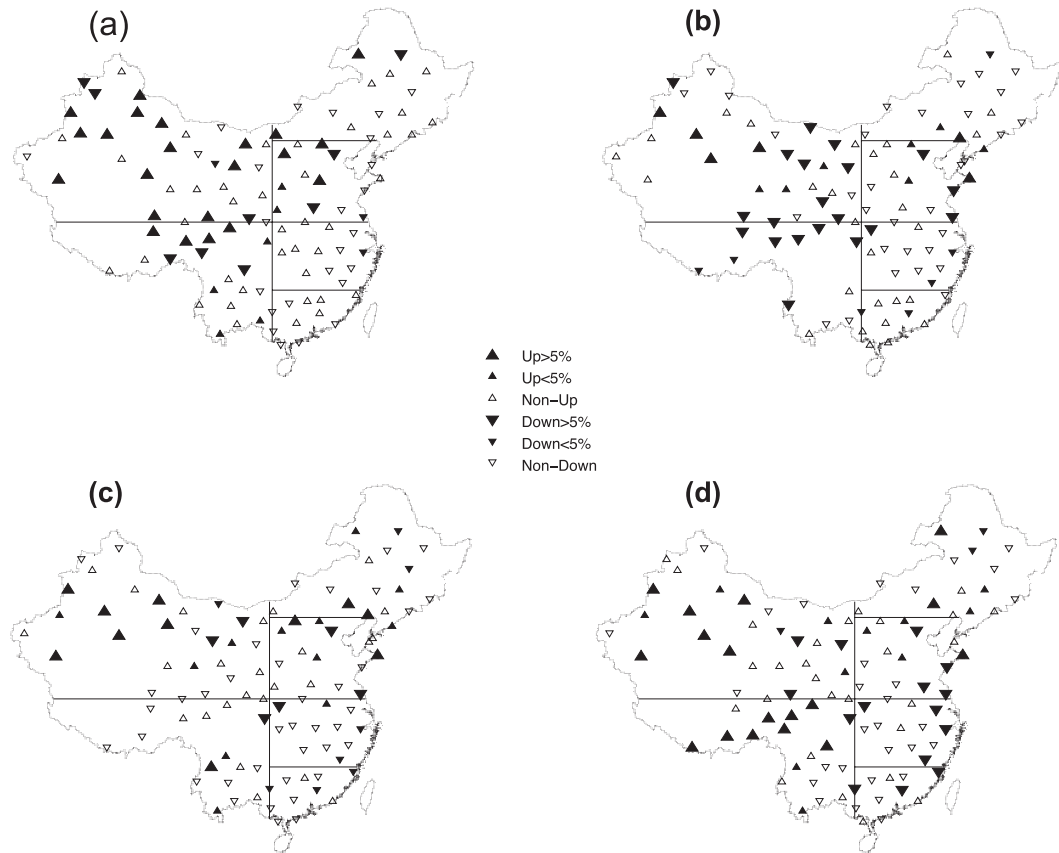


FIG. 3. Annual trends (%) in (a) PW and RH at (b) 850, (c) 700, and (d) 500 hPa for the period 1979–2005. Up (down) triangles indicate positive (negative) trends. Filled symbols indicate trends that are significant at the 95% confidence level. The larger (smaller) symbols denote relative trends with magnitude of greater (less) than 5%.

a. Annual trends

Figure 3a shows the trends of PW at each station for the period of 1979–2005. There is a general increasing trend in PW at most of the stations. Stations with magnitude of trend greater than 5% are located in northwestern China, and the magnitudes of increasing trend between 0% and 5% are seen in northern China and northeastern China. Stations with magnitude of decreasing trend of greater than 5% are rare, however. These results are partially consistent with those of surface–200-hPa integrated water vapor over 1970–90 (Zhai and Eskridge 1997) and PW trend during 1973–95 (Ross and Elliott 1996). Both these two previous works indicated that northwestern and northeastern China showed significant increasing trend in PW during the considered period. In our analysis the increasing trend is not statistically significant in northeast China from 1979 to 2005, however.

For RH at 850 hPa, the trends are not very similar to those of PW (Fig. 3b). In northwestern China, there are 12 stations showing significant decreasing trends and 9 stations with significant increasing trends. Six stations in

southwestern China show significant decreasing trends in RH at 850 hPa. Most of the stations in the rest of the region exhibit no significant trends in RH at 850 hPa, however. Several stations in northwestern China show increasing trends in RH at 700 hPa, which is similar to the results for RH at 500 hPa. Dai (2006) showed that there was an increasing trend in surface RH in northwestern China, and our results show that the increase in RH is similar to that in the lower to midtroposphere in the same region.

To evaluate the mean trends in PW and RH at 850, 700, and 500 hPa in each region, the annual mean fields and their trends are calculated and are presented in Table 1. It is interesting that there is generally an increasing trend in PW in the northern part of China and decreasing trend in the southern part of China, which is consistent with what we have shown in Fig. 2a. Only the trends in northwestern and southwestern China are significant at the 95% confidence level, however, with magnitudes of 4.8% and -2.6% , respectively.

To compare the trends in RH at different pressure levels, vertical profiles of trends in RH for each region are shown in Fig. 4. The RH in southwestern China

TABLE 1. Regionally averaged annual and seasonal trends in PW for 1979–2005. For each class, the first column is the absolute values of trends (mm) and the second column is the relative values of trends (%). Numbers in boldface denote trends that are significant at the 95% confidence level.

| Region | Region name | Annual | Summer | Winter |
|--------|-------------|--------------|-------------|-------------|
| R1 | Northwest | 0.5 | 4.7 | 3.81 |
| R2 | Southwest | -0.46 | -2.6 | 0.49 |
| R3 | Northeast | -0.31 | 2.2 | 3.34 |
| R4 | North | 0.41 | 2.1 | 5.91 |
| R5 | Central | -0.11 | -0.3 | 1.21 |
| R6 | South | 0 | 0 | 2.41 |
| | | | | 4.9 |
| | | | | -1.63 |
| | | | | -5.1 |

presents a significant decreasing (increasing) trend at 850 (500) hPa. Central China and northwestern China show significant decreasing and increasing trends of RH, respectively, at the three levels.

b. Seasonal trends

Figure 5 shows the PW trends for each station in summer and winter over the period 1979–2005. As compared

with the annual trends, seasonal trends in PW are much more distinguishable. In summer, most of the stations over China show significant increasing trends in PW, and the magnitudes of the trends are greater than 5%. In winter the results are totally reversed, however. Most of the stations show significant decreasing trends with magnitudes greater than 5% in PW in winter. Therefore, China becomes wetter (drier) in summer (winter) because of the increasing (decreasing) of PW. Considering the PW trends of each region, it is shown in Table 1 that northwestern, northeastern, and northern China have significantly increasing PW in summer with magnitudes of 27.6%, 17.3%, and 21.4%, respectively, during the period 1979–2005. Winter PW in northwestern, northeastern, southwestern, and northern China show significant decreasing trends with magnitudes of -24.1%, -7.8%, -18.9%, and -26.5%, respectively. These findings in China are similar to the discovery (Robinson 2000) that water vapor in the United States showed decreasing signal in winter in the past several decades. Note that what we have documented in the 1979–90 period is also

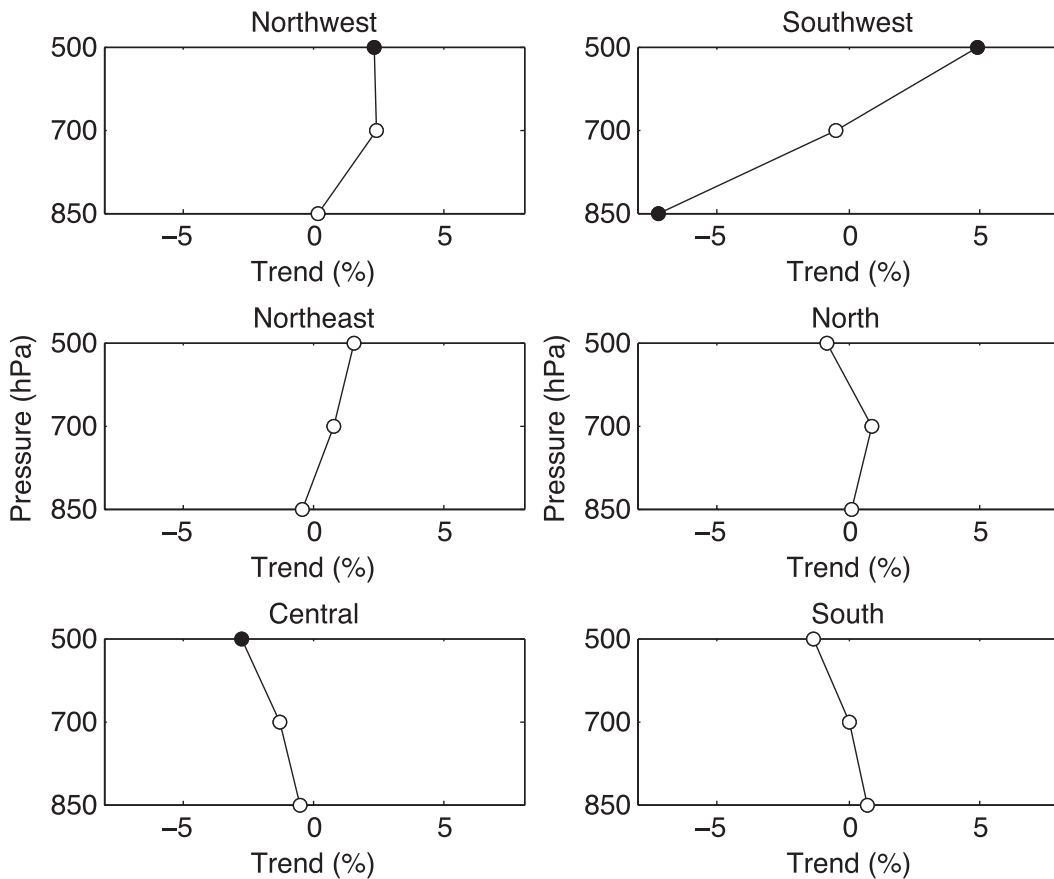


FIG. 4. The vertical profile of annual trend (%) in RH at 850, 700, and 500 hPa for the six regions. Filled circles denote trends that are significant at the 95% confidence level.

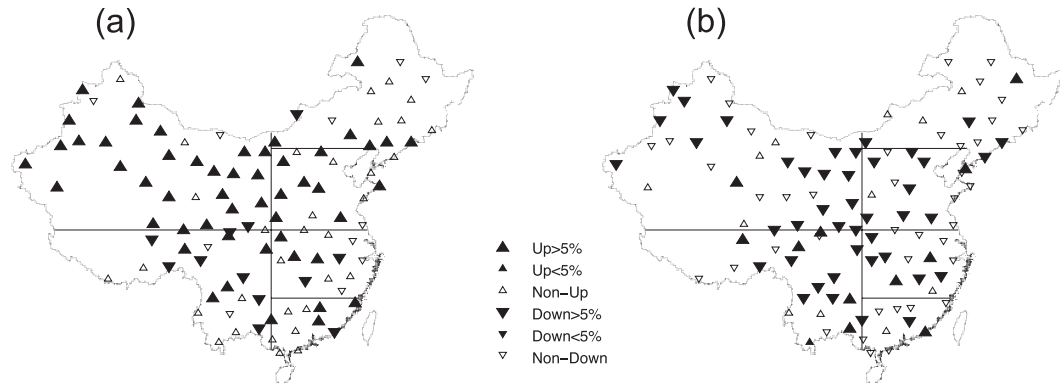


FIG. 5. Seasonal trends (%) in PW for (a) summer and (b) winter for the period 1979–2005. Up (down) triangles indicate positive (negative) trends. Filled symbols indicate the trends are significant at 95% confidence level. The larger (smaller) symbols denote absolute trends with magnitude of greater (less) than 5%.

similar to the findings in Zhai and Eskridge (1997) that the percentage of PW increased in summer over China from 1970 to 1990. The increasing trend in winter in Zhai and Eskridge (1997) is significantly different from our result, however, showing a decrease of water vapor after the 1990s.

Table 2 summarizes the seasonal trends of RH at 850 hPa for each region in summer and winter. In summer, southwestern and southern China show significant decreasing and increasing trends in RH, respectively. Table 3 shows that 700-hPa RH in southwestern and northern China have increasing trends in summer and those in southwestern China have decreasing trends in winter. For trends in RH at 500 hPa, both southwestern China (in summer) and northwestern China (in winter) showing increasing trends (Table 4).

It is of interest to consider the two trends in PW and RH in different seasons together. Recall that the definition of RH is the ratio of actual vapor pressure to the saturated vapor pressure. If RH in both seasons remain steady and the actual vapor pressures or dewpoint temperatures are higher (lower) in summer (winter), then it implies that the free atmosphere would be warmer (cooler) in summer (winter). The changes in PW in different seasons are similar to those in dewpoint temperature in the United States that are moistening in summer and drying in winter (Robinson 2000). The steadiness of

annual RH in some regions of China is very similar to the nonsignificant changes of mean RH over the globe, tropics, and Northern Hemisphere (Willett et al. 2008). Significant seasonal variations in RH can still be found in some studies, however; we cannot rule out the seasonal dependency of RH. We consider this to be evidence of seasonally dependent feedbacks of water vapor from the temperature changes of land surface and the free atmosphere. These connections will be discussed in the next section.

c. Trends in SFT and FAT

To explore this possible correlation between trends in water vapor and temperature over China, the trends of SFT and FAT in different seasons (summer and winter) over six regions for the period 1979–2005 are evaluated and are shown in Fig. 6. There is an overall increasing trend in SFT over China. In particular, the trend in winter has a larger magnitude than that in summer, which is inconsistent with the finding of decreasing PW and a constant RH. Our result is consistent with the finding in Piao et al. (2010). Of interest is that there is a significant warming signal indicated by the positive trend in FAT over the lower to midtroposphere in northwestern China in summer but no trend in winter over the northern part of China (Fig. 6). The warming magnitude in summer is very small, however, with ~ 10 m

TABLE 2. As in Table 1, but for RH at 850 hPa for 1979–2005.

| Region | Region name | Annual | | Summer | | Winter | |
|--------|-------------|-------------|-------------|-------------|-------------|-------------|-------------|
| R1 | Northwest | 0.2 | 0.1 | 0.9 | 0.4 | 0.7 | 1.3 |
| R2 | Southwest | -5.3 | -7.2 | -3.7 | -4.9 | -6.8 | -9.2 |
| R3 | Northeast | -0.4 | -0.2 | -1.7 | -2.9 | -1.3 | -2.4 |
| R4 | North | 0.1 | 0.1 | 0.9 | 1.5 | 0.7 | 1.5 |
| R5 | Central | -0.3 | -0.5 | 0.3 | 0.4 | 0.1 | 0.2 |
| R6 | South | 0.6 | 0.7 | 1.7 | 2.1 | 0.3 | 0.4 |

TABLE 3. As in Table 1, but for RH at 700 hPa for 1979–2005.

| Region | Region name | Annual | | Summer | | Winter | |
|--------|-------------|--------|------|------------|------------|-------------|-------------|
| R1 | Northwest | 1.0 | 2.4 | 1.1 | 2.4 | -1.3 | -3.1 |
| R2 | Southwest | -0.3 | -0.4 | 1.4 | 1.9 | -1.8 | -3.0 |
| R3 | Northeast | -0.4 | -0.8 | -0.7 | -1.2 | -1.6 | -2.9 |
| R4 | North | 0.4 | 0.9 | 1.6 | 2.9 | -0.1 | -0.1 |
| R5 | Central | -0.8 | -1.3 | -0.3 | -0.5 | -0.2 | -0.4 |
| R6 | South | 0 | 0.3 | 1.3 | 1.8 | -0.9 | -1.4 |

TABLE 4. As in Table 1, but for RH at 500 hPa for 1979–2005.

| Region | Region name | Annual | | Summer | | Winter | |
|--------|-------------|-------------|-------------|------------|-------------|------------|------------|
| | | | | | | | |
| R1 | Northwest | 1.0 | 2.3 | 0.5 | 1.1 | 2.1 | 5.2 |
| R2 | Southwest | 2.5 | 4.9 | 1.4 | 10.1 | -1.6 | -3.9 |
| R3 | Northeast | 0.6 | 1.5 | 0.2 | 0.5 | 1.5 | 3.5 |
| R4 | North | -0.4 | -0.9 | 0.1 | 0.2 | 0 | 0 |
| R5 | Central | -1.4 | -2.7 | -0.8 | -0.5 | -1.9 | -4.5 |
| R6 | South | -0.6 | -1.3 | 2.3 | 3.9 | -2.6 | -8.8 |

as compared with a mean thickness of ~ 4000 m. No significant trend in FAT is found over other regions either in summer or in winter.

5. Discussion

The influences of climatic change on water vapor are complex problems related to the climatological behavior of temperature, soil moisture, surface runoff, agriculture, and even underground water. The above sections show a series of results for the variations and trends in PW, RH, SFT, and FAT. The topics we will discuss are 1) What are the fundamental causes underlying the changes of water vapor and other related factors? And 2) What are the correlations among the changes of PW, RH, and precipitation over China?

As was presented in the previous sections, positive trends are found in both SFT and PW over most of China, especially in the northern part of China in summer. Similar findings were also documented by plenty of previous studies that show that the increasing water vapor (especially water vapor near the surface) was strongly coupled with a similar trend in SFT in warm seasons (Zhai and Eskridge 1997; Vincent and Mekis 2006; Wang and Gaffen 2001). We are interested in the inconsistency in winter of strong warming coming with significant decreasing of PW, however. Our concern is why and how the strong warming of surface in winter was associated with the decrease in water vapor in the northern part of China. The considered dominant factors effecting PW amount in the atmosphere are evaporation, water availability at the surface, atmospheric circulation, and the mean temperature of the atmosphere. SFT is one of the key factors that may affect the evaporation processes. The warming of land surface would positively enhance evaporation in the regions where water source is not limiting. Because of the small amount of precipitation (as compared with that in summer), frozen soil, and/or runoffs in winter, however, the limited availability of water resource would possibly reduce the water vapor evaporation rate, which likely leads to the warming of the surface. Thus, a negative feedback loop between the SFT and water vapor availability has likely been established in the past decades

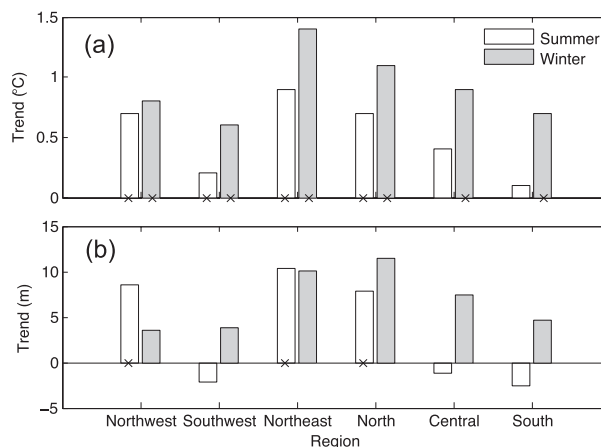


FIG. 6. Seasonal trends (white is summer, and gray is winter) in (a) surface temperature and (b) 850–500-hPa thickness for the six regions during the period 1979–2005. The times signs at the bottom of the bars indicate trends that are significant at the 95% confidence level.

and will possibly continue. This hypothesis could make a well-understood interpretation of why air is becoming drier (decreasing of PW) and the surface is becoming warmer in winter in the northern part of China.

The differences between the long-term trends in PW and RH may be partially caused by precipitation, because precipitation is a process that balances the water contents at the surface and in the atmosphere. More PW is not always associated with more precipitation, since high PW value does not necessarily mean the high RH that is a prerequisite for the occurrence of precipitation. Because precipitation is strongly affected by water vapor transportation, frontal cyclones, and convective systems, however, we tend to deduce that the long-term trend of regional precipitation may still be related to the trend of either RH or PW. In general, high (lower) PW is related to more (less) precipitation over China (Zhai and Eskridge 1997). They also found that the increase (decrease) in PW water is associated with an increase (decrease) in precipitation in most regions over China from 1970 to 1990, although this result is obtained from the correlation analysis in which precipitation trends are really small. Ren et al. (2000) used station observations to document the increasing trends in summer precipitation in northwestern, northeastern, and southern China since the 1990s. Piao et al. (2010) have confirmed the increasing precipitation in northwestern and southern China, but they suggested a negative trend in precipitation in northeastern China because of the intensively decreasing precipitation in that region. These findings are consistent with the trends of PW and RH at 500 hPa over these regions in this study.

The processes of change seen in SFT, PW, and precipitation vary in different regions, however. In northwestern China, the rise in temperature (both SFT and FAT) causes the glaciers to melt and thus enhances evaporation (Piao et al. 2010) and increases precipitation, which is likely driving the increase in PW and RH. Meanwhile, because of the increasing population and the development of agriculture in northwestern China, more and more underground water is being consumed by irrigation. This may increase water vapor through evapotranspiration, if water resource is not limiting. Therefore, the increasing water vapor may well be occurring at the expense of glacier extent and underground water exhaustion. If these reductions are sustained, water availability in the future could become limited. By contrast, the warming and decreased precipitation accompanied by increased drought (Piao et al. 2010) is the main cause of decreased water vapor in northeastern China. Such changes in PW in northern and northeastern China are expected to be related to the weakening of the eastern Asian summer monsoon that transports water vapor from the ocean to the northern part of China (Ding et al. 2008; Piao et al. 2010). On the other hand, aerosols may also be a factor that decreases the precipitation in northern China where dense population and heavy industrial emissions exist (Zhao et al. 2006). We conclude that the long-term trends in PW and RH are associated with many processes, including warming, precipitation, atmosphere circulation, and even anthropogenic factors. Further studies may focus on quantifying the effect of each factor contributing to such trends.

6. Summary

This study documented the long-term trends of PW and RH at 850, 700, and 500 hPa over different regions in China for the period of 1979–2005 on the basis of data derived from twice-daily radiosonde observations. Evidence from annual trends of PW implied a significant increasing trend in the northern part of China and a decreasing trend in wet areas (especially southern China). Annual trends in RH at the three levels (850, 700, and 500 hPa) showed no significant change over China.

Seasonal trends of PW and RH showed that water vapor has increased in summer and decreased in winter in the northern part of China. These results cannot be explained by surface temperature changes, which have larger increasing magnitude in the cold season than in the warm season, indicating the existence of other related physical processes.

The long-term trends of 850–500-hPa thicknesses are calculated to compare with the long-term trends of PW and RH. It is shown that relatively strong land surface

warming, possible limited water availability, and unchanged FAT co-occur with decreasing winter PW and may be causal factors. In general, long-term trends of RH and PW are found to have a certain relationship with the trends of precipitation in most regions of China.

Acknowledgments. This study is supported by the Chinese National Public Benefit Research Foundation of Meteorology (Grant GYHY200906025) and the National Nature Science Foundation of China under Grants 40921160380 and 40975059. The authors thank three anonymous reviewers for their valuable comments and helpful suggestions toward the improvement of the paper.

REFERENCES

- Dai, A., 2006: Recent climatology, variability, and trends in global surface humidity. *J. Climate*, **19**, 3589–3606.
- Ding, Y. H., Z. Y. Wang, and Y. Sun, 2008: Inter-decadal variation of the summer precipitation in East China and its association with decreasing Asian summer monsoon. Part I: Observed evidences. *Int. J. Climatol.*, **28**, 1139–1161.
- Durre, I., C. N. Williams, X. Yin, and R. S. Vose, 2009: Radiosonde-based trends in precipitable water over the Northern Hemisphere: An update. *J. Geophys. Res.*, **114**, D05112, doi:10.1029/2008JD010989.
- Elliott, W. P., 1995: On detecting long-term changes in atmospheric moisture. *Climatic Change*, **31**, 349–367.
- Gaffen, D. J., T. P. Barnett, and W. P. Elliott, 1991: Space and time scales of global tropospheric moisture. *J. Climate*, **4**, 989–1008.
- Held, I. M., and B. J. Soden, 2000: Water vapor feedback and global warming. *Annu. Rev. Energy Environ.*, **25**, 441–475.
- Karl, R. T., S. J. Hassol, C. D. Miller, and W. L. Murray, Eds., 2006: Temperature trends in the lower atmosphere: Steps for understanding and reconciling differences. Climate Change Science Program and the Subcommittee on Global Change Research Synthesis and Assessment Product 1.1, 164 pp. [Available online at <http://www.climatechange.gov/Library/sap/sap1-1/finalreport/sap1-1-final-all.pdf>]
- Kiehl, J. T., and K. E. Trenberth, 1997: Earth's annual global mean energy budget. *Bull. Amer. Meteor. Soc.*, **78**, 197–208.
- McCarthy, M. P., H. A. Titchner, P. W. Thorne, S. F. B. Tett, L. Haimberger, and D. E. Parker, 2008: Assessing bias and uncertainty in the HadAT-adjusted radiosonde climate record. *J. Climate*, **21**, 817–832.
- , P. W. Thorne, and H. A. Titchner, 2009: An analysis of tropospheric humidity trends from radiosondes. *J. Climate*, **22**, 5820–5838.
- Philipona, R., and B. Dür, 2004: Greenhouse forcing outweighs decreasing solar radiation driving rapid temperature rise over land. *Geophys. Res. Lett.*, **31**, L22208, doi:10.1029/2004GL020937.
- , —, A. Ohmura, and C. Ruckstuhl, 2005: Anthropogenic greenhouse forcing and strong water vapor feedback increase temperature in Europe. *Geophys. Res. Lett.*, **32**, L19809, doi:10.1029/2005GL023624.
- Piao, S., and Coauthors, 2010: The impacts of climate change on water resources and agriculture in China. *Nature*, **467**, 43–51.
- Ren, G., H. Wu, and Z. Chen, 2000: Spatial patterns of changes trend in rainfall of China (in Chinese). *Quart. J. Appl. Meteor.*, **11**, 321–330.

- Robinson, P. J., 2000: Temporal trends in United States dew point temperatures. *Int. J. Climatol.*, **20**, 985–1002.
- Ross, R. J., and W. P. Elliott, 1996: Tropospheric water vapor climatology and trends over North America: 1973–93. *J. Climate*, **9**, 3561–3574.
- Simmons, A. J., K. M. Willett, P. D. Jones, P. W. Thorne, and D. P. Dee, 2010: Low-frequency variations in surface atmospheric humidity, temperature, and precipitation: Inferences from reanalyses and monthly gridded observational data sets. *J. Geophys. Res.*, **115**, D01110, doi:10.1029/2009JD012442.
- Trenberth, K. E., 1999: Atmospheric moisture recycling: Role of advection and local evaporation. *J. Climate*, **12**, 1368–1381.
- , and D. P. Stepaniak, 2003a: Covariability of components of poleward atmospheric energy transports on seasonal and interannual timescales. *J. Climate*, **16**, 3690–3704.
- , and —, 2003b: Seamless poleward atmospheric energy transports and implications for the Hadley circulation. *J. Climate*, **16**, 3705–3721.
- , A. Dai, R. M. Rasmussen, and D. B. Parsons, 2003: The changing character of precipitation. *Bull. Amer. Meteor. Soc.*, **84**, 1205–1217.
- , J. Fasullo, and L. Smith, 2005: Trends and variability in column integrated atmospheric water vapor. *Climate Dyn.*, **24**, 741–758.
- Vincent, L. A., and É. Mekis, 2006: Changes in daily and extreme temperature and precipitation indices for Canada over the twentieth century. *Atmos.–Ocean*, **44**, 177–193.
- Wang, J.-W., K. Wang, R. A. Pielke Sr., J. C. Lin, and T. Matsui, 2008: Towards a robust test on North America warming trend and PW content increase. *Geophys. Res. Lett.*, **35**, L18804, doi:10.1029/2008GL034564.
- Wang, J. X. L., and D. J. Gaffen, 2001: Trends in extremes of surface humidity, temperatures and summertime heat stress in China. *Adv. Atmos. Sci.*, **18**, 742–751.
- Willett, K. M., P. D. Jones, N. P. Gillett, and P. W. Thorne, 2008: Recent changes in surface humidity: Development of the HadCRUH dataset. *J. Climate*, **21**, 5364–5383.
- Zhai, P. M., and R. E. Eskridge, 1997: Atmospheric water vapor over China. *J. Climate*, **10**, 2643–2652.
- Zhao, C., X. Tie, and Y. Lin, 2006: A possible positive feedback of reduction of precipitation and increase in aerosols over eastern central China. *Geophys. Res. Lett.*, **33**, L11814, doi:10.1029/2006GL025959.